0031-3998/00/4803-0340
PEDIATRIC RESEARCH
Vol. 48, No. 3, 2000
Printed in U.S.A.

Real-Time Spectral Analysis of the Fetal EEG: A New Approach to Monitoring Sleep States and Fetal Condition during Labor

ISRAEL THALER, RAPHAEL BOLDES, AND ILAN TIMOR-TRITSCH

Departments of Obstetrics and Gynecology [I.T.], Rambam Medical Center, Faculty of Medicine-Technion, Israel Institute of Technology, Haifa, Israel; Misgav Ladach Maternity Hospital [R.B.], Jerusalem, Israel; and New York University Medical Center [I.T.T.], New York, NY 10016, U.S.A.

ABSTRACT

Adverse perinatal events affecting cerebral functions are a major cause of neonatal mortality, morbidity, and long-term neurologic deficit. Intrapartum fetal EEG, which records fetal brain electrical activity, provides a monitoring modality for evaluating the fetal CNS during labor. In this study, we describe a new approach to such monitoring that is based on real-time spectral analysis of the fetal EEG during labor. Fourteen pregnant women with uncomplicated term pregnancies who went into labor participated in the study. Two suction-cup electrodes were applied to the fetal scalp at the occipitoparietal or parietal region after rupture of membranes. Real-time spectral analysis was used to determine the frequency and amplitude of the fetal EEG signal. The spectral edge frequency (SEF) was calculated as the frequency below which 90% of the power in the power spectrum resides. The average EEG amplitude and the SEF were displayed using the density spectral array technique. Fetal heart rate and intrauterine pressure were also measured. Two fundamental EEG patterns were identified: high-voltage slow activity and low-voltage fast activity. The SEF was found to be an excellent index of cyclic EEG activity. Fetal heart rate demonstrated increased variability and an elevated baseline during low-voltage fast activity, whereas both parameters decreased during high-voltage slow activity. During episodes of variable decelerations in the fetal heart rate, a decrease in the SEF was observed, accompanied by an increased EEG voltage. The results obtained substantiate the presence of sleep cycles in the human fetus. This kind of cortical activity monitoring may enable rapid alertness to cerebral hypoxia and allow for prompt intervention, thereby decreasing the risk for birth asphyxia and subsequent brain damage. **(*Pediatr Res* 48: 340–345, 2000)**

Abbreviations

SEF, spectral edge frequency
DSA, density spectral array
FHR, fetal heart rate
IUP, intrauterine pressure
HVSA, high-voltage slow activity
LVFA, low-voltage fast activity

Normal function of the fetal CNS is of paramount importance to the quality of life after birth. Methods for assessing the normality or abnormality of the CNS function before birth are required to perform this sort of fetal evaluation. Fetal EEG, which records fetal brain electrical activity, can be used to measure CNS function. Methods for continuous monitoring of the fetal EEG were previously described, both in mature and premature fetuses (1, 2). Various EEG patterns were recognized, both transient and nontransient, that were found to be associated with intrapartum events and also with neurologic abnormalities at 1 y of age (3, 4). These observations were based on visual analysis of the fetal EEG records, which presented many methodologic as well as interpretative problems, precluding clinical acceptance of this monitoring modality. In recent years, automated methods for EEG scoring and coding for EEG states have been proposed (5–8). Such methods are objective and offer greater consistency of pattern recognition while facilitating processing and quantitative evaluation of large amounts of data. This approach may potentially provide for rapid alertness to cerebral hypoxia, thus enabling early clinical intervention to prevent subsequent neurologic damage. It can also be used to monitor the effect of certain drugs on the fetal CNS and permit rapid discrimination of fetal sleep states, more generally expressed as fetal behavioral cycles. This system may also be used in the neonatal period for a continual evaluation of the integrity of cerebral function.

In this study, we performed spectral analysis of the fetal EEG in an attempt to characterize patterns that reflect fetal sleep cycles and changes that may be associated with FHR decelerations during labor. Basically, two spectral parameters are derived from the native EEG: the power spectrum, displayed as the DSA, and the SEF, the highest frequency at

Received June 25, 1999; accepted April 4, 2000.
Correspondence and reprint requests: Israel Thaler, M.D., Department of Obstetrics and Gynecology, Rambam Medical Center, Haifa 31096, Israel.
Supported by the Kerenyi Perinatal Research Fund, New York, NY.

which a significant amount of power is present in the EEG. The latter has previously been used for measuring cerebral maturation in fetal lambs (9) and human neonates (10) and also for monitoring the depth of anesthesia in adults (5, 11).

METHODS

Fourteen pregnant women at term, who were admitted to the delivery room with spontaneous uterine contractions, participated in the study. The mean gestational age was 39.9 ± 1.2. The course of their pregnancy was uneventful, they were nonsmokers, and they did not take any medications during pregnancy excluding iron supplementation. The present study was approved by the local ethics committee, and each woman signed an informed consent before EEG recordings of the fetus and the neonate. Recordings of fetal EEG were obtained after rupture of the amniotic membranes, during the active stage of labor. No drugs or medications were given before or during the recordings.

Two custom-made circular EEG electrodes with a central metal probe were applied to the fetal scalp at the occipital-parietal or the parietal region. The minimal separation between the electrodes was 4 cm. The suction-cup electrodes, made of silicone rubber, were attached by applying a continuous negative pressure by use of a continuous pressure pump (Fig. 1). The FHR was recorded by use of a scalp electrode, and the IUP was recorded by using a fluid-filled polyvinyl catheter that was inserted into the uterine cavity. The other end of the catheter was attached to a pressure transducer (Hewlett Packard 1290C). An FHR monitor (Hewlett Packard 8040A) processed both parameters. All signals were sampled at a frequency of 250 Hz, then stored and displayed by a Cerebro-Trac 2500 (SRD Medical Ltd., Shorashim, Israel). The Cerebro-Trac employs a real-time fast Fourier transform (FFT) algorithm for calculating the power spectrum of the fetal EEG. Epoch length of EEG acquisition was 4 s. Band-pass filters were set at 1.5–30 Hz, and amplifier sensitivity was 200 μV. The FFT allows the presentation of the EEG signal in terms of the relative power of the various frequencies of which it is composed. The frequencies were then displayed by using the DSA technique. This method presents each frequency component (or spectrum) as a row of frequency elements with each element displayed by a pixel or square mosaic unit. The brightness of a given pixel represents the relative power present at the corresponding frequency element in the EEG. In this manner, a spectral time record appears as a black and white or gray scaled image (Fig. 2) in which a given spectrum takes up only a single row of pixels. This makes it particularly amenable to side-by-side plotting with the other trended variables (*i.e.* FHR and IUP). The DSA display facilitates discrimination between the different wavebands: 0.3 to 3 Hz (delta), 4 to 7 Hz (theta), 8 to 11 Hz (alpha), 12 to 14 Hz (sigma), and 15 to 32 Hz (beta).

The SEF indicating the highest dominant frequency in the EEG signal (*i.e.* the frequency below which 90% of the power resides) was also displayed (Fig. 2). This complemented a separate display of EEG amplitude, allowing the user to distinguish between amplitude and frequency changes in the EEG. A running window (4–9 s) of the raw EEG signal was also displayed for ascertaining an artifact-free recording. The video display showed the trended EEG spectrum and amplitude, the real-time EEG record, and the trended display of additional parameters (*e.g.* FHR, uterine contraction, and maternal blood pressure) as was previously described (12). The numerical values of all recorded variables were displayed above their respective time plots (12). The user controlled the system via a menu-driven keypad. In this manner, the total elapsed time to be displayed, ranging from 5 min to several hours, could be determined. Each external event (*e.g.* fetal stimulation) or

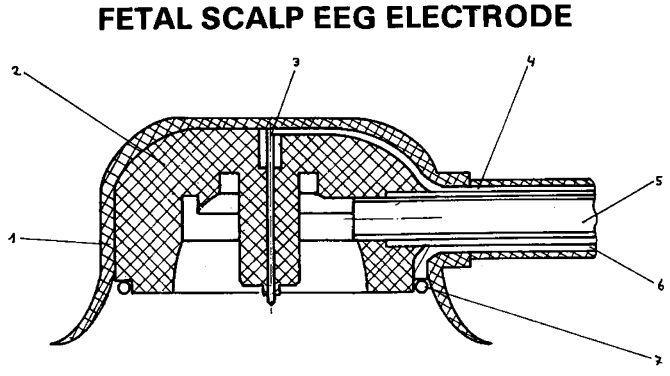

Figure 1. Schematic presentation of the fetal scalp EEG electrode. (*1*) Rubber silicone sheath, (*2*) plastic filling material, (*3*) central stainless steel electrode, (*4*) EEG lead, (*5*) negative pressure chamber, (*6*) reference lead, (*7*) circular metal probe.

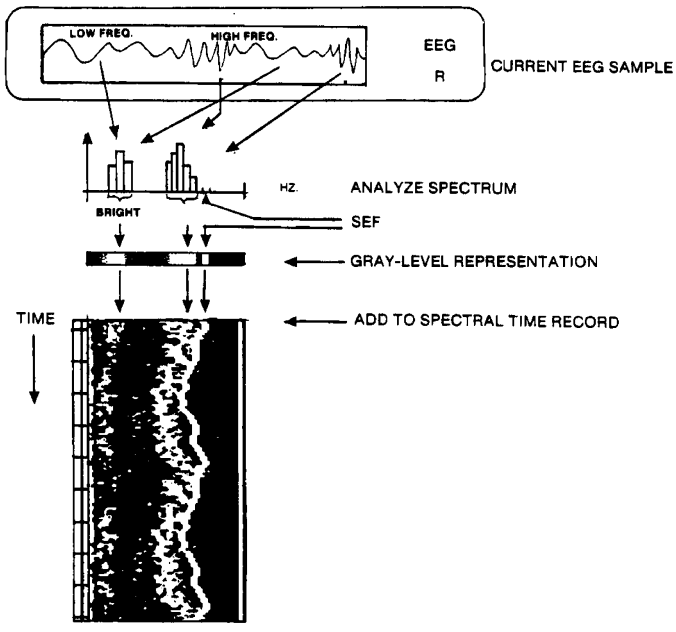

Figure 2. Spectral analysis of the fetal EEG displayed in DSA format. Spectral analysis determines the relative power at each frequency in a given EEG sample. The power spectrum is shown as a bar graph with each bar representing a given frequency. The height of the bar is proportional to the power at that frequency. In the DSA display format, each bar is replaced by a mosaic. The brightness of a mosaic, determined by the density of dots in it, represents the height of the corresponding bar graph. Thus, each sample of the EEG is represented by a row of gray-scale mosaics, and the DSA spectral time record displays a stack of such rows, forming a gray-scale picture. The SEF can readily be observed in the spectral time plot.

changes introduced to the setup of the system were also printed.

RESULTS

All women had uneventful delivery and normal outcome. The mean birth weight was 3294 ± 242 g. The mean Apgar score at 5 min was 9.1 ± 0.99. The mean arterial cord pH at delivery was 7.39.1 ± 0.027. There were no admissions to the neonatal intensive care unit. In three women, several episodes of variable FHR decelerations were observed during the recordings.

Two fundamental EEG patterns were readily identified in all the recordings: HVSA and LVFA. The SEF was found to be highly effective in differentiating between the two patterns.

Figure 3 shows a typical DSA recording from a normal fetus during labor, demonstrating an epoch of low-voltage high-frequency activity. In the lower axis of the display, the actual time is marked every 5 min, and the ticks are spaced 1 min apart. The lower channel shows the spectral time record and clearly displays the SEF. The scale extends from 0 to 30 Hz. The amplitude of the EEG signal (expressed in microvolts) is shown adjacent to the frequency channel. Because only two electrodes were applied, the EEG parameters were only displayed on one side of the trace. Changes in frequency and amplitude are readily observed on the trended display. Uterine contractions are shown in the upper channel. The scale extends from 0 to 100 mm Hg. The adjacent trace shows the FHR expressed in bpm. A large acceleration can be observed at the beginning of the trace, followed by an increased baseline variation.

FHR accelerations were typically associated with periods of LVFA. There was no relationship between uterine contractions and the SEF or DSA.

The 90% SEF was found to be an excellent index of cyclic EEG activity. This is shown in Figure 4, demonstrating a transition from LVFA to HVSA. The FHR during fast EEG activity demonstrated increased short-term and long-term variability. The baseline declined during transition into slow EEG activity, and heart rate variability, both long-term and short-term, substantially decreased. The SEF during fast EEG activity was in the range of the sigma waveband, whereas during slow EEG activity, it fell into the range of the theta and alpha bands.

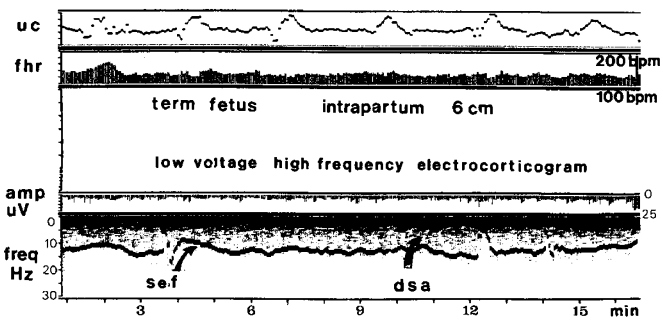

Figure 3. Typical course of the EEG power spectrum demonstrating an LVFA epoch displayed as DSA and the SEF (*lower channel*) in a normal fetus during labor. The EEG amplitude is displayed in microvolts next to the lower channel. The *upper two channels* show simultaneous recordings of FHR and uterine contractions (*UC*). Note the increased FHR variation and the presence of FHR acceleration.

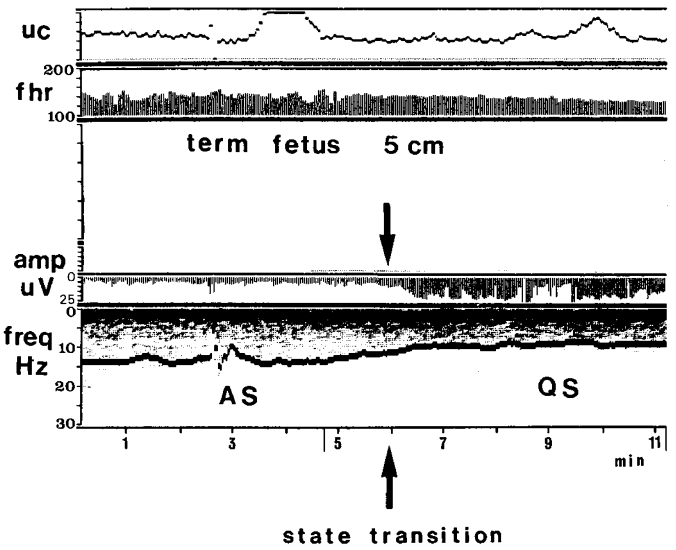

Figure 4. Power spectrum of the fetal EEG during labor displayed as DSA and the SEF, demonstrating a transition (denoted by *arrows*) from LVFA to HVSA. The recording was taken at 5-cm cervical dilatation. During HVSA, FHR declined and there was a substantial decrease in FHR variation (*FHR channel*, second from top). LVFA corresponds to active behavioral state (*AS*), whereas HVSA corresponds to quiet behavioral state (*QS*).

Table 1 summarizes the data obtained from all 14 fetuses, demonstrating for every fetus the number of episodes of each sleep cycle as well as the total and the mean duration of each cycle. The sleep cycles at the beginning and end of the recordings were excluded. Also shown are the birth weight and gestational age at delivery.

Table 2 summarizes the data for all the 14 fetuses combined. Altogether, there were 34 episodes of LVFA lasing 1390 min (mean ± SD, 40.88 ± 16.93 min) and 37 episodes of HVSA lasting 922.15 min (mean ± SD, 24.92 ± 8.27 min). On average, LVFA was present 60.1% of the time, whereas HVSA was present 39.9% of the time.

Figure 5 demonstrates changes in the EEG during episodes of variable decelerations in the FHR. The recording was performed during LVFA. The scale of spectral time record (lower channel) extends from 0 to 15 Hz. Whenever FHR declined below 100 bpm, it was marked by dots rather than by vertical bars (arrows). During those epochs, the scale extended from 0 to 100 bpm. During variable decelerations, a marked increase in EEG voltage (arrows) and a decline in the SEF were observed, and the SEF shifted from the alpha to the theta waveband. The intensity of the DSA display increased, particularly at the lower frequencies (delta and theta bands) under the SEF mark. There were no changes in the beat-to-beat variability during these episodes, and the cord pH at delivery was within normal range.

DISCUSSION

The goal of intrapartum fetal monitoring is to prevent fetal mortality and morbidity, which may occur during labor from

Table 1. *No. of episodes of each sleep cycle (LVFA and HVSA) during the recording for each fetus in the study is shown, together with mean duration and range*

			LVFA			HVSA		
	Week	Birth weight	Episodes	Range (min)	Mean (min)	Episodes	Range (min)	Mean (min)
1	39	2990	2	37–69.5	53.25	2	20.5–36.5	28.5
2	40	3165	2	26–58.5	42.25	3	22.5–32.5	34.3
3	41	3010	3	25–63	46.5	4	11.5–19.5	16
4	41	3215	3	18.5–61.5	42.7	3	23.25–34.5	27.25
5	39	3380	3	24.5–47.8	33.3	3	9.5–15.5	12.6
6	38	2940	3	15.5–79	53	3	28.3–33	30.2
7	40	3240	3	25–54	36.2	3	27.3–36	33.5
8	40	3510	2	42.5–56.5	54.5	2	16.3–34.5	25.4
9	41	3205	2	26.5–66	46.25	2	32–44.2	38.1
10	41	3565	3	22–45.5	31.3	3	23–29.5	25.7
11	38	3150	2	35.5–41	38.25	2	16.5–17	16.75
12	39	3450	2	20–58	39	2	25.75–38.25	32
13	42	3670	2	29–33.75	31.38	2	25.5–28.5	27
14	40	3630	2	27.5–34	30.75	3	11–27.25	20.08

Cycles at the beginning and end of the recording session were excluded. Birth weight and gestational age at delivery (in weeks) are also shown.

Table 2. *Summary of the total and mean (±SD) duration the 14 fetuses spent in each sleep cycle (LVFA and HVSA)*

	LVFA	HVSA
No. of episodes	34	37
Total duration (min)	1390	922.15
Mean duration (min)	40.88 ± 16.93	24.92 ± 8.27
% of time	60.1	39.9

The total no. of episodes of each cycle is also shown, and the percentage of time spent in a particular cycle.

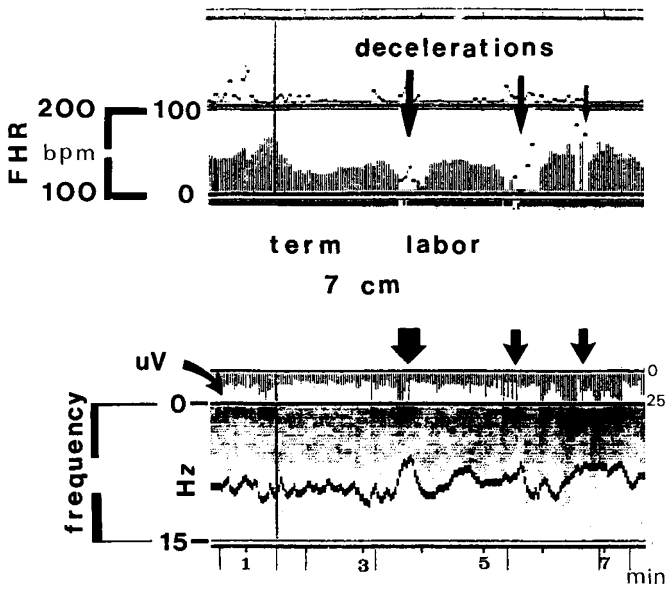

Figure 5. Changes in the fetal EEG during episodes of variable heart rate decelerations (*upper arrows*). The FHR is depicted by vertical bars whenever it was above 100 bpm and by dots whenever it declined below 100 bpm (*second channel from top*). During decelerations, there was a marked increase in EEG voltage (marked by the *lower set of arrows*), whereas the SEF declined. The increase in power was particularly dominant at the lower frequencies (delta and theta bands).

factors other than trauma. The morbidity that gives cause for greatest concern is hypoxic brain damage, leading to subsequent neurologic syndromes including mental retardation, cerebral palsy, and epilepsy. Fetal EEG is the only method available for direct monitoring of fetal cerebral function in labor. The difficulty of using this parameter lies in the clinical impracticalities of using the voluminous unprocessed trace generated by conventional EEG recorders. This requires skilled interpretation and is not suitable for prolonged recording or monitoring. Methods that would reduce the fetal EEG into a more manageable format could be suitable for routine clinical practice. Furthermore, the relation between the fetal EEG and other trended variables (*e.g.* FHR, IUP) during labor could then be determined in a more practical manner.

One such method is power spectrum analysis, which determines the frequency and amplitude composition of the fetal EEG signal. It can detect clinically important EEG changes with high sensitivity and reliability (6, 13). Power spectral analysis has been used for performing quantitative analysis of changes in frequency components of the fetal EEG. In this manner, information on the maturational changes in the electrocorticogram waveforms of the fetal lamb (7, 14), baboon (8), and guinea pig (15) was obtained.

This technique was also used to study changes in the electrocorticogram of the fetal lamb under hypoxic conditions (16). However, comparison of a large number of power spectra is both cumbersome and impractical when performing long-term fetal EEG monitoring during labor.

In this study, a new method for monitoring fetal cortical activity during labor was presented that is based on real-time spectral analysis of the fetal EEG. To enable the simultaneous display of this information along with trended records of other fetal monitored signals, the DSA and the SEF of the EEG were used. Statistical trend estimation methods were able to detect and quantify trends in monitored parameters (17). In this manner, the user could readily distinguish between amplitude and frequency changes in the fetal EEG and correlate such changes with other trended variables (*e.g.* FHR, IUP) or external events (*e.g.* fetal acoustic stimulation) that can be displayed simultaneously.

The results of this study show that the SEF is effective in demonstrating the cyclic behavior of the fetal EEG by discrim-

inating between HVSA and LVFA. The presence of behavioral states in the human fetus was previously suggested on the basis of FHR patterns, fetal movements, and, when present, the regularity or irregularity of fetal breathing movements (18). In a more comprehensive study that also included fetal eye movements in the classification criteria, behavioral states similar to those in the neonate were shown to exist in the human fetus (19). Specifically, four states were recognized: state 1F, characterized by quiescence, absent eye movements, and stable heart rate; state 2F, characterized by frequent and periodic gross body movements associated with FHR accelerations, wider oscillation bandwidth of the FHR, and eye movements that are continually present; state 3F, characterized by the absence of gross body movements, continually present eye movements, and a stable heart rate (but with higher oscillation bandwidth than in 1F); and state 4F, characterized by continual body movements and trunk rotations, continually present eye movements, and unstable heart rate with large and prolonged accelerations. State 1F represents quiet sleep, whereas state 2F represents active sleep. States 3F and 4F represent awake states and are infrequent in occurrence (19, 20).

The present study shows for the first time that human fetal sleep states can be classified by real-time spectral analysis of the EEG. This substantiates, in a direct manner, the existence of behavioral cycles in the human fetus.

The EEG pattern in Figure 3 and the first part of Figure 4 demonstrates LVFA (denoted by AS). This behavioral state, associated with increased heart rate variation and the presence of heart rate accelerations, corresponds to state 2F as previously described (19). The latter part of Figure 4 (denoted by QS) demonstrates HVSA and is associated with stable heart rate with small oscillation bandwidth (*i.e.* decreased heart rate variability and absence of accelerations). This corresponds to state 1F.

When the results of this study are compared with those of Timor-Tritsch *et al.* (18), who distinguished between quiet and active states on the basis of visual analysis of FHR baseline and variability in relation to fetal movements, an interesting resemblance emerges. The mean duration of the quiet state in the latter study was 22.8 min compared with a mean duration of 24.9 min spent in HVSA in the present study. The respective figures for the active state and LVFA in the two studies were 39.5 and 40.9 min. This also supports the association between sleep cycles defined by the electrical activity of the brain and behavioral states, defined by FHR patterns and gross body movements.

Monod and Pajot (21), who performed polygraphic recordings in human neonates born near term, could distinguish between two different sleep states: active sleep with flat or rhythmic EEG tracing and quiet sleep with a tracé alternant on the EEG pattern. These investigators recorded the electrooculogram in addition to the EEG and noted that during quiet sleep, eye movements are absent, whereas during active sleep, rapid eye movements are continually present. Therefore, quiet sleep and active sleep have a global overlap with no-rapid eye movement sleep (non-REM sleep) and rapid eye movement sleep (REM sleep), respectively. They also calculated that the human neonate spends 60% of the sleeping time in REM sleep and 40% in non-REM sleep. This is almost identical with our findings during LVFA and HVSA (60.1 and 39.9%, respectively), suggesting that LVFA represents REM sleep whereas HVSA represents non-REM sleep.

In chronic fetal sheep studies, the LVFA was shown to be associated with rapid eye movements, whereas during HVSA, eye movements were absent (22). Therefore, LVFA and HVSA are considered to represent REM sleep and non-REM sleep, respectively, and this can be correlated with the study by Nijhuis *et al.* (19) who visualized fetal eye movements by using real-time ultrasound imaging.

The SEF has also been shown to provide a sensitive measure of the oscillations between HVSA and LVFA in the electrocorticogram of the fetal lamb (9). In the fetal baboon, the SEF was demonstrated to be a good discriminator of EEG patterns (8). This EEG parameter was also useful in measuring cerebral maturation in the newborn infant, demonstrating a significant correlation with gestational age (10). This study also demonstrated that the SEF was significantly higher in active sleep compared with quiet sleep.

The SEF can also offer rapid alertness to potentially ominous trends by employing continuous cerebral monitoring during labor. This is demonstrated in the changes that we have observed during variable decelerations in the FHR that are related to brief compression of the umbilical cord. During such episodes, there was a substantial increase in EEG amplitude and a decrease in the SEF, *i.e.* a transition into HVSA. There was a relative increase in power distribution at lower frequencies (delta and theta bands). These changes were of short duration and generally coincided with the changes in FHR. When polygraph EEG recordings were obtained during labor from human fetuses with evident clinical and biochemical signs of hypoxia and acidosis at delivery, a decrease in the frequency and wave amplitude was observed (23). In cases of severe fetal hypoxia and acidosis, an isoelectric line appeared. During severe fetal asphyxia induced by prolonged cord occlusion in the fetal lamb, the EEG also demonstrated different patterns. When asphyxia was induced in the near-term fetal lamb by brief repetitive umbilical cord occlusions, lowering the pH to 6.83, a progressive suppression of the EEG was observed associated with epileptiform and spike activity (24). During partial umbilical cord occlusion for 90 min (lowering the pH to 6.82), the electrocorticogram of the fetal lamb was profoundly suppressed and seizure activity was documented after release of occlusion in all surviving animals (25). Our observations demonstrate that during short episodes of cord compression insufficient to cause fetal acidemia (based on pH measurements in cord blood at delivery and the lack of changes in heart rate variability), the fetal EEG reflects a state of stimulation rather than suppression (Fig. 5).

The main advantage of the system is the ability to perform continuous cerebral monitoring during labor that can be readily interpreted. Methods for continuous cerebral monitoring were previously sought. A system that would improve the interpretation of the EEG after birth was proposed, based on amplitude-integrated EEG (aEEG) that was recorded on a slow-running paper (26). This cerebral function monitor reflects trends in averaged levels of cerebral activity. It has been shown

to be predictive of gestational age (26) and of neurologic status in the asphyxiated neonate (27). On this cerebral monitor, neonates born within 24 h of a nonreactive nonstress test showed subtle changes involving reversion to more immature patterns and lack of sleep cycling (28).

The prognostic value of aEEG was assessed in full-term asphyxiated infants during the first 6 h after birth (29). All infants who demonstrated a continuous aEEG background pattern of normal voltage survived and had normal outcome. Continuous but extremely low voltage patterns or flat (mainly isoelectric) tracings were associated with high neonatal mortality. In those who survived, a severe handicap was subsequently diagnosed. Most infants who demonstrated a burst-suppression pattern either died or survived with severe handicap. Only 21% were healthy at follow up. Altogether, the type of background pattern recorded within the first 6 postnatal h in the aEEG tracings predicted outcome correctly in 91.5%. In another study, the aEEG was used to assess infants with neonatal encephalopathy. Results were compared with neurodevelopmental outcome assessed at 18 to 24 mo of age. The aEEG, performed within 12 h of birth, predicted outcome with a sensitivity of 1.0, a specificity of 0.82, positive predictive value of 0.85, and a negative predictive value of 1 (30). A "plain" EEG recorded before 48 h of life was used to predict the neurologic outcome in infants with hypoxic-ischemic encephalopathy after acute fetal distress (31). The EEG had an excellent sensitivity rate (94.7%) but a less satisfactory specificity rate (68.4%). The aEEG, therefore, seems to be a feasible technique for identifying infants at high risk for subsequent brain damage who might benefit from interventionist treatment after birth asphyxia. However, the aEEG employs signal-processing techniques such as band-pass filtering and amplitude and time compression and rectification (26), adequate for screening purposes but insufficient to obtain detailed information regarding amplitude and frequency components embedded in the signal. In contrast, automated scanning of the EEG by spectral analysis as described in this study offers both accuracy and ease of interpretation and, when effectively displayed, provides a sensitive and reliable monitor of cortical activity (5, 9, 10). The system can also be applied postnatally, so that central neurologic adaptation can be evaluated both in preterm and term newborns.

The SEF has also been used to study the effect of drugs and medications on the EEG, to monitor the depth of anesthesia in adults (5, 11), and to study the effects of drugs and chemicals in laboratory animals and fetal lambs (32, 33). Further studies are required to characterize the effects of clinically relevant perturbations such as hypoxia and drug therapies on the fetal CNS function. It may also facilitate the study of the ontogeny of sleep states under normal and abnormal conditions.

REFERENCES

1. Bernstine RL, Borkowski WJ, Price AH 1955 Prenatal fetal electro-encephalography. Am J Obstet Gynecol 70:623–630
2. Rosen MG, Scibetta JJ, Chick L, Borgstedt AD 1973 An approach to the study of brain damage: the principles of fetal electroencephalography. Am J Obstet Gynecol 115:37–47
3. Rosen MG, Scibetta JJ, Hochberg CJ 1970 Human fetal electroencephalogram: 3. Pattern changes in presence of fetal heart rate alterations and after use of maternal medications. Obstet Gynecol 36:132–140
4. Borgstedt AD, Rosen MG, Chick L, Sokol RJ, Bachelder L, Leo P 1975 Fetal electroencephalography. Relationship to neonatal and one-year developmental neurological examinations in high-risk infants. Am J Dis Child 129:35–38
5. Rampil IJ, Sasse FJ, Smith NT, Hoff BH, Fleming DC 1980 Spectral edge frequency–a new correlate of anesthetic depth. Anesthesiology 53:512–517
6. Levy WJ, Shapiro HM, Maruchak G, Meathe E 1980 Automated EEG processing for intra-operative monitoring. Anesthesiology 53:223–236
7. McNerney ME, Szeto HH 1990 Automated identification and quantification of four patterns of electrocortical activity in the near-term fetal lamb. Pediatr Res 28:106–110
8. Myers MM, Stark RI, Fifer WP, Grieve JH, Leung K, Schulze KF 1993 A quantitative method for classification of EEG in the fetal baboon. Am J Physiol 265:R706–R714
9. Szeto HH 1990 Spectral edge frequency as a simple quantitative measure of the maturation of electrocortical activity. Pediatr Res 18:289–292
10. Bell AH, McClure BG, McCullagh PJ, McClelland RJ 1991 Spectral edge frequency of the EEG in healthy neonates and variation with behavioural state. Biol Neonate 60:69–74
11. Schwender D, Daunderer M, Mulzer S, Klasing S, Finsterer U, Peter K 1996 Spectral edge frequency of the electroencephalogram to monitor "depth" of anaesthesia with isoflurane or propofol. Br J Anaesth 77:179–184
12. Pearlman A, Gurman G 1985 Toward unified monitoring system during anesthesia. Int J Clin Monit Comput 2:21–27
13. Rampil IJ, Smith NT 1983 The use of computer-generated numbers in interpreting the EEG. In: Prakash A (ed) Computing in Anesthesia and Intensive Care. Martinus Nijhoff Press, The Hague, pp 211– 226
14. Szeto HH, Vo TD, Dwyer G, Dogramajian ME, Cox MJ, Senger G 1985 The ontogeny of fetal lamb electrocortical activity: a power spectral analysis. Am J Obstet Gynecol 153:462–466
15. Umans JG, Cox MJ, Hinman DJ, Dogramajian ME, Senger G, Szeto HH 1985 The development of electrocortical activity in fetal and neonatal guinea pig. Am J Obstet Gynecol 153:467–471
16. Symmes D, Prichard JW, Mann LI 1970 Spectral analysis of fetal sheep EEG during hypoxia. Electroencephalogr Clin Neurophysiol 29:511–515
17. Beneken JEW, Blom JA, Saranummi N 1983 Accuracy in trend detection. In: Gravenstein JS (ed) An Integrated Approach to Monitoring. Butterworths, London, pp 133–144
18. Timor-Tritsch IE, Dierker LJ, Hertz RH, Deagan C, Rosen MG 1978 Studies of antepartum behavioral states in the human fetus at term. Am J Obstet Gynecol 132:524–528
19. Nijhuis JG, Prechtl HFR, Martin CB, Bots RSGM 1982 Are there behavioral states in the human fetus? Early Hum Dev 6:177–195
20. Griffin RL, Caron FJM, van Geijn HP 1985 Behavioral states in the human fetus during labor. Am J Obstet Gynecol 152:828–833
21. Monod N, Pajot N 1965 Le sommeil du nouveau-né et du prématuré. I. Analyse des études polygràphiques (mouvements oculaires, respiration et E.E.G) chez le nouveau-né à terme. Biol Neonat 8:281–307
22. Dawes GS, Fox HE, Leduc BM, Liggins GC, Richards RT 1972 Respiratory movements and rapid eye movement sleep in the fetal lamb. J Physiol 220:119–143
23. Djelmis J, Drazancic A, Durrigl V, Ivansenic M 1988 The effect of fetal hypoxia and acidosis on the changes in fetal electroencephalogram during labor. Am J Perinatol 5:177–185
24. De Haan HH, Gunn AJ, Williams CE, Gluckman PD 1997 Brief repeated umbilical cord occlusions cause sustained cytotoxic cerebral edema and focal infarcts in near-term fetal lambs. Pediatr Res 41:96–104
25. Ball RH, Parer JT, Caldwell LE, Johnson J 1994 Regional blood flow and metabolism in ovine fetuses during severe cord occlusion. Am J Obstet Gynecol 171:1549–1555
26. Verma UL, Archbald F, Tejani NA, Hanwerker SM 1984 Cerebral function monitoring in the neonate. I: Normal patterns. Develop Med Child Neurol 26:154–161
27. Archbald F, Verma UL, Tejani NA, Handwerker SM 1984 Cerebral function monitor in the neonate. II: Birth asphyxia. Develop Med Child Neurol 26:162–168
28. Shiffman R, Tejani N, Verma U 1988 Correlation of cerebral function monitoring with non-reactive non-stress test. Acta Obstet Gynecol Scand 67:297–300
29. Hellstrom-Westas L, Rosen I, Svenningsen NW 1995 Predictive value of early continuous amplitude-integrated EEG recordings on outcome after severe birth asphyxia in full-term infants. Arch Dis Child Fetal Neonatal Ed 72:F34–F38
30. Al Naqeeb N, Edwards AD, Cowan FM, Azzopardi D 1999 Assessment of neonatal encephalopathy by amplitude-integrated electroencephalography. Pediatrics 103:1263–1271
31. Selton D, Andre M 1997 Prognosis of hypoxic-ischemic encephalopathy in full-term newborns–value of neonatal electroencephalography. Neuropediatrics 28:276–280
32. Jones RD, Sheets LP, Mueller RE 1995 Methods for screening drug and chemical effects in laboratory rats using computerized quantitative electroencephalography. Vet Hum Toxicol 37:521–527
33. Szeto HH, Cheng PY, Wu DL, Soong Y 1994 Effects of the delta-opioid agonist, [D-Pen2,D-Pen5]-enkefalin, on fetal lamb EEG. Pharmacol Biochem Behav 49:795–800